38th International Electric Vehicle Symposium and Exhibition (EVS38)
Göteborg, Sweden, June 15-18, 2025

Comparing Battery Costs Between Charging Infrastructure Alternatives

Lars Lindgren[1], Anders Grauers[2]
[1]*Chalmers University, lars.lindgren@chalmers.se*
[2]*Chalmers University, anders.grauers@chalmers.se*

Executive Summary

Different electrification infrastructure concepts for electric vehicles can be difficult to compare economically because they use batteries in different ways. Often, there are options with frequent high-power short-time charging or slower charging with deeper charging cycles. This paper presents a method for comparing the battery-related costs associated with these options and applies it to long-haul trucks using different types of charging infrastructure. The battery related costs can then be compared to the cost differences between different infrastructure options to identify the best overall solution. Many existing battery aging models do not fit this type of investigation well, either requiring too much information and computation time, or do not cover e.g. the approximate dynamic behavior of the battery. To address this, we introduce a novel model designed to approximate how different use cases influence battery-related costs for a generic battery type, rather than modeling the behavior of any specific battery pack.

Keywords: Batteries, Modeling & Simulation, Electric Vehicles, Heavy Duty electric Vehicles & Buses, Fast and Megawatt charging infrastructure

1 Introduction

This work stems from difficulties in several system studies, e.g. [1, 2] in consistently and realistically modeling and comparing battery-related costs between charging system options. These options result in different battery usage, particularly in relation to cycle depth distribution, charging power, and charging patterns. Commonly used battery models are either too detailed or make unwarranted simplifications. Detailed models often require unknown parameter values and are computationally intensive. Common problems with simplified models are that they e.g. estimate the damage from fast charging based on the average or RMS-current over the charging phase. It is easy to construct counterexamples that show that these models are not realistic in some cases. The presented model can estimate the costs associated with specific battery usage patterns and charging solutions, even before selecting vehicle models or battery solutions. This capability is crucial for developing long-term infrastructure strategies and policies.

2 Battery degradation model for cost estimation

The battery model suggested in this paper is illustrated in Figure 1. The model is intended to be as simplified as possible while still capturing the important behavior for a rough techno-economic optimization of a system.
The model's input consists of the battery's charging and discharging power as a function of time for representative time intervals, typically one or a few days. The power is then filtered through an equivalent circuit battery model, designed to capture properties of the battery usage which relates to different aging mechanisms. The results are used to calculate battery degradation through two mechanisms:

- A degradation term per unit of time based on an internal voltage and current in the battery.
- A degradation term per discrete charging cycle that depends on the minimum and maximum equivalent state of charge (SOC) in the cycle.

Combined with a model of acceptable battery degradation at the end of its economic life and an economic model considering interest rates and other factors, the overall cost of the battery use case can be estimated.
This model does not include any thermal dynamics; it is assumed that the battery heating/cooling system is designed so that the battery can be kept close to an ideal average operating temperature at all times during operation. The assumption that the battery almost always operates in a reasonable temperature range is a reasonable assumption for commercial vehicles that have large batteries with slow temperature dynamics and that operate for long predictable periods at a time.
The lack of a thermal model makes it harder to compare the results with laboratory tests that are typically performed at well-defined temperatures. It also limits the accuracy of the results, but makes it much easier to apply the model to system design problem at the concept development stage, before the vehicle models have been designed or selected. To properly include the thermal dynamics would include modeling the cost associated with thermal systems of different performance levels and the optimal control of these.
Since the model is intended for use in an optimization loop, it should have a few properties:

- It should not fail if the battery is misused; instead, it should give a very sharp increase in battery degradation when the battery is used outside normal operating conditions, as this will guide the optimization algorithm to acceptable operating regions. The model accuracy is not important outside normal operating conditions since they will not be selected, i.e. it does not matter if the battery would last e.g. 10 minutes or 10 seconds in a unrealistic extreme operating point, as long as the aging is so fast that the optimization will never converge in that operating point.
- It should be reasonably fast to compute, since it will be calculated many times.

The selected parameters in this model are intended to roughly approximate NMC batteries, but the model has not yet been systematically fitted to any data on battery degradation. The goal is to keep the model as generic as possible.

2.1 Circuit model to model battery dynamics

The electrochemical dynamics of a battery is complicated and in the general case is modeled as a set of PDE:s. In order to make a model that is understandable and computationally fast, it is preferable to express it as a circuit model. The circuit model used is intended mainly to help model battery aging in a simple way, by filtering the current to useful signals for degradation calculation. In addition, it is also used to estimate losses. If accurate loss estimation is important, a separate circuit model can be used only for loss calculation, or the model may need to be more complex. A real battery has different dynamics in the anode, cathode, and electrolyte. The dynamics is partially caused by diffusion and, therefore, requires Warburg diffusion elements to describe. These cannot be described exactly by a conventional finite lumped circuit model.
For our purposes, the circuit model needs to do three things:

- Filter out high-frequency shallow charging/discharging cycles in the range above about 0.1 Hz to 0.01 Hz. It is well-known that the ripple current and fast current variations have a very small impact on battery aging. This filtering is done with C_1 in the model. To some extent, C_1 can be considered to represent the double layer capacitance in the battery cells. Therefore, it is modeled as a linear capacitor according to Equation 1. Making C_1 linear also helps to reduce the computation time.
- Capture the increased degradation as a result of, e.g. sustained fast charging. In frequency ranges between, e.g. 0.01 Hz and 0.0001 Hz the cycles are long enough to cause significant ion transport, but not so slow that the battery is close to equilibrium. This puts extra stress on the battery that needs to be modeled, this is done with C_2.
- Model the overall bulk state of charge; this is modeled by the sum of the charge in $C_1 + C_2 + C_3$ where C_3 has the majority of the capacity and represents the capacity of the bulk of the electrode material.

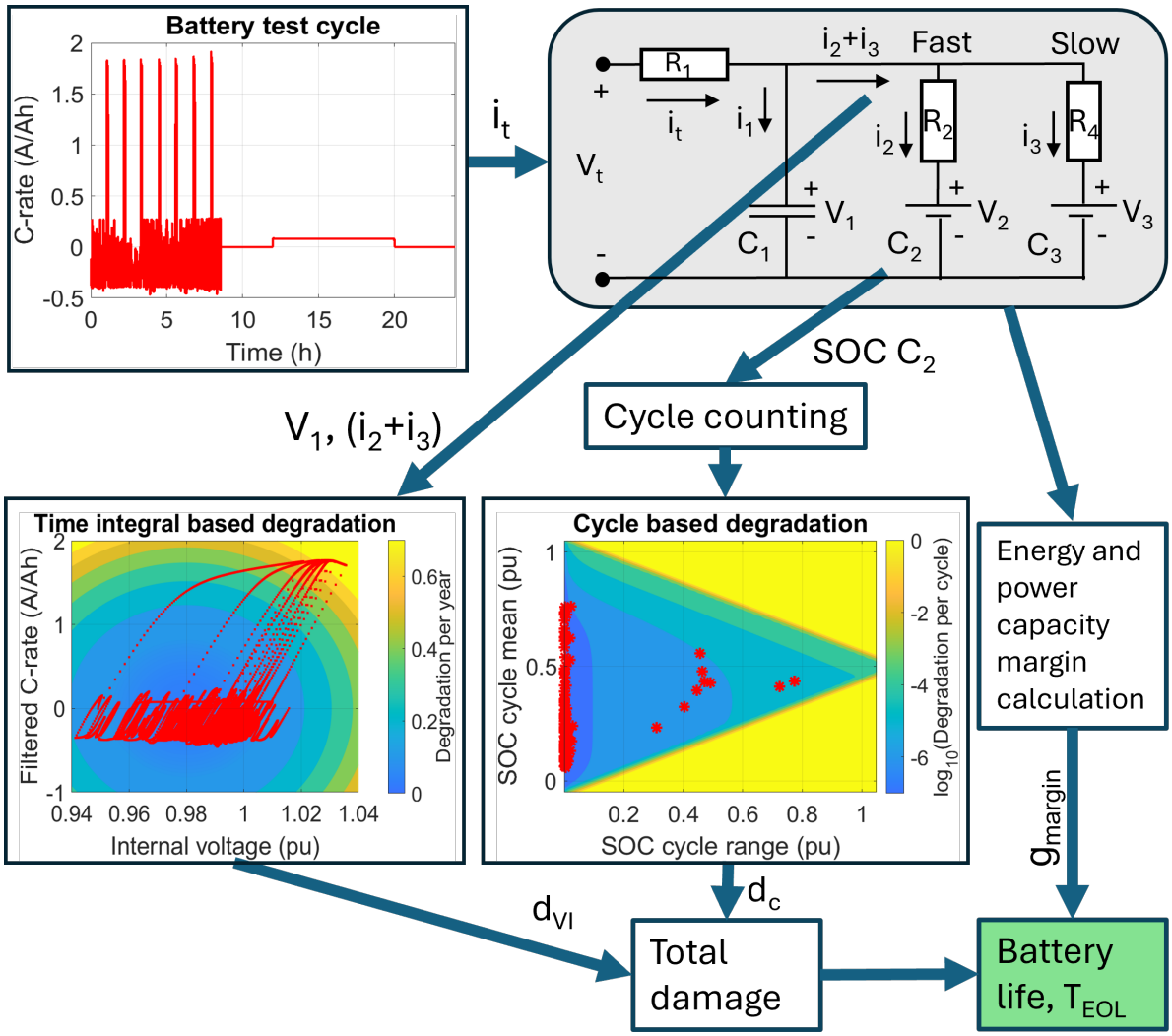

Figure 1: The battery model for cost estimation. The red lines/points which are shown in the diagrams are for the "Fast ch. 5 min every 75 km" case.

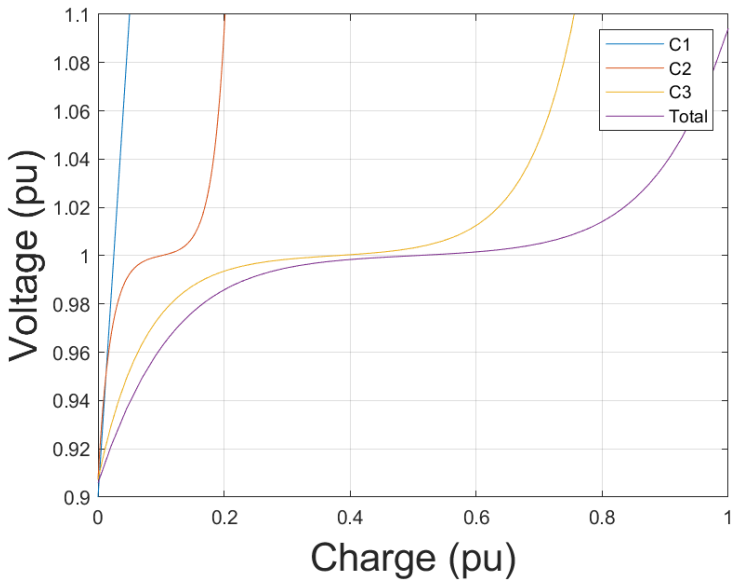

Figure 2: The relation between voltage and charge used for the different parts of the model

Table 1: Parameters.
1C current is defined as the current that fully charge the battery in one hour.

Parameter	Symbol	Value	Unit
Circuit model			
Max Voltage	V_{max}	1.1	p.u.
Min Voltage	V_{min}	0.9	p.u.
Resistance at terminals	R_1	0.025	Fraction loss at 1C current
Resistance to C_2	R_2	0.025	Fraction loss at 1C current
Resistance to C_3	R_4	0.042	Fraction loss at 1C current
Fraction of the total charge storage in the capacitor over the voltage range	C_1	5%	Fraction of the total charge.
Charge storage in the first OCV over the voltage range	C_2	20%	Fraction of the total charge.
Charge storage in the second OCV over the voltage range	C_3	75%	Fraction of the total charge.
OCV center	p_1	0.5	-
OCV sharpness	p_2	10	-
OCV voltage scaling	p_3	800	-
OCV voltage offset	p_3	1	-
Battery life calculation			
Nominal capacity loss at EOL	p_{EOL}	0.2	-
Degradation knee exponent	$p_{EOL\ exp}$	2	-
Economic calculation			
Battery capacity	E_{cap}	-	kWh
Mass per kWh	m	7.28	kg/kWh
Battery cost per kWh	c_{batt}	208	EUR/kWh
Energy cost	c_{energy}	0.2	EUR/kWh
Cost of battery mass in application case	c_{mass}	5	EUR/kg
Discount rate	$r_{discount}$	15	$\%/year$
Cost of failure to deliver or absorb energy	c_{fail}	10	EUR/kWh
Time integral based degradation			
Extreme voltage degradation exponent multiplier	p_{d1}	120	-
Extreme voltage degradation scaling	p_{d2}	$8 * 10^{-8}$	p.u./year
Voltage with minimum degradation	$V_{min\ d}$	0.98	p.u.
Voltage scaling for degradation	p_{d3}	10	p.u.
Current scaling for degradation	p_{d4}	0.33	p.u.
Scaling for degradation by voltage and current	p_{d5}	0.9	p.u./year
Minimum calendar degradation rate	d_{min}	0.024	1/year
Cycle based degradation			
Cycle degradation scaling	p_{c1}	$5 * 10^-6$	
High SOC cycle degradation offset	p_{c2}	0.815	
High SOC cycle degradation exponent multiplier	p_{c3}	20	
Low SOC cycle degradation offset	p_{c4}	0.077	
Low SOC cycle degradation exponent multiplier	p_{c5}	30	
Extreme SOC cycle degradation offset	p_{c6}	0.0347	
Extreme SOC cycle degradation exponent multiplier	p_{c7}	300	
SOC range degradation exponent multiplier	p_{c8}	2	
Degradation proportional to cycled energy	p_{c9}	0.03	

Other degradation models often try to include the effects of e.g. fast charging by making the degradation a function of e.g. the average or RMS charging current over a charging cycle, it is, however, trivial to generate charging cycles with identical RMS-Current that have very different degradation in reality. For this reason, it seems necessary to use a dynamic model to capture the dynamic behavior.
For example, compare charging a battery at 1 C for 600 seconds followed by 30 C for 60 seconds with alternating 10 seconds at 1 C followed by 1 second at 30 C and so on for 660 seconds. The latter case is obviously much better, but has exactly the same RMS-current.
Especially for optimization of electric road layouts, it is important to get the degradation caused by dynamic behavior right, since electric roads give rise to very complex charging patterns, and an optimization algorithm can easily exploit flaws in the degradation model that give unrealistically low degradation in corner cases.
The open circuit voltage (OCV) curve for C_1 is linear.

$$V_1 = SOC_1 * (V_{max} - V_{min}) + V_{min} \tag{1}$$

Since C_2 and C_3 are intended to model the charging and discharging of different parts of the battery electrodes, they are modeled with a non-linear open circuit voltage (OCV) curve

$$V_i = sinh((SOC_i - p_1) * p_2)/p_3 - p_4, i \in 2, 3 \tag{2}$$

as shown in Figure 2.
The circuit is simulated with forward Euler integration and one second time step. This gives acceptable computation times for testing but can be improved significantly, for example, by using longer time steps for C_2 and C_3.

2.2 Time integral based degradation

It is generally known that the calendar aging of batteries is strongly dependent on the state of charge. The cell is optimized to work around the nominal voltage and high or low SOC gives a voltage that deviates from the nominal voltage. The resulting electrochemical potentials within the battery cell cause unwanted side reactions that result in degradation.

The model for time integral based degradation describes an aging rate, which varies during the battery usage cycle and is integrated to give the damage over the cycle, d_{VI}.

$$d_{VI} = p_{d5}\left(\int_0^T p_{d2} e^{(p_{d1}\ |(V_1(t)-1)|)^2} dt + \int_0^T (e^{(p_{d3}(V_1(t)-V_{min\ d}))^2 + (p_{d4}*(i_2(t)+i_3(t)))^2} - 1)dt + T\ d_{min}\right) \tag{3}$$

This proposed equation was found by iterative adjustment to obtain results that meet expected battery degradation. The resulting degradation rate can be illustrated as a 3D map, which can be seen in the lower left corner of Figure 1.

The degradation processes are chemical processes whose reaction rates are governed by the Arrhenius equation, which has an exponential relation between the electrochemical potential and reaction rate. This makes it reasonable to assume an exponential function. The current also contributes to the degradation by, among other mechanisms, causing voltage drops that make the electrochemical potential inhomogeneous.

The first integral in Equation 3, gives very fast degradation at extreme voltages outside the normal range. It has little impact in normal operation, but gives a very short expected battery life at extreme voltages. When the model is used in an optimization loop where battery life is included in the cost function, this acts as soft voltage limits. By using soft voltage limits, with a gradient towards normal operation, instead of hard limits, it is much easier for an outer optimization loop to find parameters that give operation in the normal voltage range.
The second integral gives zero degradation at zero current and a voltage of $V_{min\ d}$ and is increasing exponentially further from this point. The last term, $T \cdot d_{min}$, sets the minimum calendar aging when the battery is stored at $V_{min\ d}$.

2.3 Cycle based degradation

Battery degradation is often described in terms of the number of charging/discharging cycles the battery can withstand between different SoC levels. This is convenient in many applications, fits well with typical testing procedures, and captures battery degradation due to mechanical stress and cracking in the electrodes. Observe that in this model the degradation due to battery cycling is split between ”Time integral based degradation” and ”Cycle based degradation”.

Mechanical stress is mainly introduced because the inflow and outflow of ions cause the electrodes to swell and shrink. Cracks in the electrodes cause different degradation mechanisms, such as disconnecting electrode material, exposing more surface area to formation of solid electrolyte interface which binds up cyclable lithium, and so on. In a real cell, there are different modes of mechanical stress that contribute to mechanical degradation such as:

- Variation in the volume of the bulk electrode.
- Difference in swelling in different parts of the macroscopic electrode material.
- Difference in swelling on the surface and center of the individual microscopic electrode grain.

The two last modes are exacerbated by fast charging and discharging, since the ion concentrations in the electrodes do not have time to equalize.

In this model, we want to capture all these different modes of cycle-based degradation with one single cycling model. The cycle-based degradation model is based on the SOC variations of C_2 in the circuit model that represents the state of charge of the electrode surface. This makes cycles with high C-rate look deeper than they are, and therefore capture the increased damage from cycling with high C-rate.

Since the model is intended to be used in complex scenarios where small cycles can be overlaid on larger cycles, we need a way to go from a messy time series of SOC values to a list of cycles with the lowest and highest SOC values for each. For this we use the classical rain-flow counting method. [3]

The degradation map used for cycle-based degradation can be seen in the lower middle part of Figure 1. This map shows the rate of degradation given by Equation 4a. This degradation rate is based on the integration of exponential functions over the SOC range of the cycle, and then we sum the degradation of all N cycles during the test sequence. The first two integrals set up increasing degradation towards the upper and lower parts of the SOC-range. The parameters are selected to give more degradation in the upper part of the SOC range than in the lower part, since this is often observed in real batteries. The next two integrals are basically the same but with parameters set to give a really low battery life if operated outside the specified SOC range of 0 to 100%. The fifth integral increases the degradation for cycles with a large SOC range regardless of the mean SOC level. The last integral represents a fixed degradation per cycled amount of energy. With the current parameters, the last integral gives only a small contribution to the overall degradation and could possibly be removed.

The integrals in Equation 4a can be solved analytically, resulting in Equation 4b, this is what is actually implemented in the simulation code.

$$
\begin{aligned}
d_C = p_{c1} \sum_{n=0}^{N} \Bigg(& \int_{SOC2_{min}(n)}^{SOC2_{max}(n)} p_{c3} * e^{p_{c3}(x-p_{c2})} dx + \int_{SOC2_{max}(n)}^{SOC2_{min}(n)} p_{c5} * e^{p_{c5}(-x-p_{c4})} dx + \\
& + \int_{SOC2_{min}(n)}^{SOC2_{max}(n)} p_{c7} * e^{p_{c7}(x-1-p_{c6})} dx + \int_{SOC2_{max}(n)}^{SOC2_{min}(n)} p_{c7} * e^{p_{c7}(-x-p_{c6})} dx + \\
& + \int_{0}^{SOC2_{max}(n)-SOC2_{min}(n)} p_{c8} e^{p_{c8}x} dx + \int_{0}^{SOC2_{max}(n)-SOC2_{min}(n)} p_{c9} dx \Bigg)
\end{aligned}
\tag{4a}
$$

$$
\begin{aligned}
d_C = p_{c1} \sum_{n=0}^{N} \Big(& e^{p_{c3}(SOC2_{max}(n)-p_{c2})} - e^{p_{c3}(SOC2_{min}(n)-p_{c2})} + \\
& + e^{p_{c5}(-SOC2_{min}(n)-p_{c4})} - e^{p_{c5}(-SOC2_{max}(n)-p_{c4})} + \\
& + e^{p_{c7}(SOC2_{max}(n)-1-p_{c6})} - e^{p_{c7}(SOC2_{min}(n)-1-p_{c6})} + \\
& + e^{p_{c7}(-SOC2_{min}(n)-p_{c6})} - e^{p_{c7}(-SOC2_{max}(n)-p_{c6})} + \\
& + e^{p_{c8}(SOC2_{max}(n)-SOC2_{min}(n))} - 1 + \\
& + p_{c9}(SOC2_{max}(n) - SOC2_{min}(n)))
\end{aligned}
\tag{4b}
$$

2.4 Battery life calculation

To predict the expected battery life in a specific application, we need to consider a few things:

- The total degradation over one test cycle is calculated here simply as $d_{VI} + d_C$. In reality, degradation of different types cannot necessarily be added directly, but it is a common simplifying assumption.
- How much reduction in power and energy capacity that is acceptable while still fulfilling the requirements of the test cycle, this is calculated as the minimum of the margin in energy storage, discharging power and charging power:

$$g_{margin} = \min(1-(SOC2_{max}-SOC2_{min}), \min_{t\in[0\ t_{max}]}(1-P(t)/P_{max}(t)), \min_{t\in[0\ t_{max}]}(1-P(t)/P_{min}(t)) \tag{5}$$

  Where $\min(1-(SOC2_{max}-SOC2_{min})$ is the energy capacity margin, $P_{max}(t)$ and $P_{min}(t)$ is the maximum and minimum power that the battery can deliver while the terminal voltage stays in the specified voltage range, calculated for each timestep. Observe that this is a simplification, since there is no guarantee that this power could be sustained for the required time.
- A way to translate the total amount of degradation into the remaining energy and power capacity, often the power capacity decreases faster than the energy capacity, but here it is assumed that both decrease at the same rate. The degradation parameters are designed so that the degradation of 100% results in the remaining capacity of $p_{\ EOL} = 80\%$. The function from degradation to remaining capacity can be very different between different batteries and operating conditions. Often there is a rapid loss of capacity first followed by a slower loss of capacity and then a knee after which the capacity falls rapidly again. The knee is important to model; therefore, the remaining capacity is modeled as $E_{cap}(1-(d_{VI}+d_C)^{p_{\ EOL\ exp}})$ where $p_{\ EOL\ exp} = 2$, basically a quadratic loss of capacity with increased degradation. This can be rearranged to

$$d_{max} = \left(\frac{g_{margin}}{p_{\ EOL}}\right)^{1/p_{\ EOL\ exp}} \tag{6}$$

  where d_{max} is the maximum degradation allowed while the battery is still useful in the application.
- Calculate the total battery life by multiply the test cycle time by the ratio of allowable degradation to the degradation from one cycle.

$$T_{EOL} = T_{test}\frac{d_{max}}{d_{VI}+d_C} \tag{7}$$

Once the battery life has been calculated, the yearly battery-related cost can be calculated.

$$F_{cost}(E_{cap}, p_{Popt}) = E_{cap}\cdot(c_{batt}\mathrm{F}_{\text{annuity}}(T_{EOL}(E_{cap}, p_{Popt}), r_{discount}) + m\ c_{mass}) + \\ + c_{energy}E_{loss\ per\ year}(E_{cap}, p_{Popt}) + c_{fail}\cdot(E_{notDelivered}+E_{NotCharged}) \tag{8}$$

Where $E_{cap}c_{batt}\mathrm{F}_{\text{annuity}}(T_{EOL}(E_{cap}, p_{Popt}), r_{discount})$ is the annual cost of paying the investment at the given interest rate.
$E_{cap}\,m\ c_{mass}$ is the cost in e.g. lost payload capacity from the battery mass mE_{cap}.
The last term $c_{fail}\cdot(E_{notDelivered}+E_{NotCharged})$ is an extra cost applied if the battery cannot follow the test cycle based on the size of the energy deviation. After optimization, it is normally zero.
The battery life in the examples in Section 3 is assumed to be separate from that of the vehicle. Therefore, the overall cost of the vehicle does not factor into the cost equation. In reality, it is often practical if the vehicle life is the same as the battery life, or an integer multiple of the battery life so that used batteries do not need to be moved between vehicles unnecessarily.

2.5 Rescaling for Energy vs. Power optimization

The model presented so far describes a single type of battery that scales in size but otherwise has the same properties. In order to compare different charging solutions with different requirements in terms of energy storage and power capabilities, it is necessary to consider batteries that have different compromises between energy-optimized and power-optimized cell types, cooling, and interconnections. One way to do this would be to try to model a number of existing such compromises, optimize each, and then select the cheapest alternative. However, the way that is used in this work is to do an interpolation of the available compromises. To do this, the parameter p_{Popt} is defined such that 0 is a fully energy-optimized battery and 1 is a fully power-optimized battery. The parameter values presented so far represent the case of $p_{Popt} = 0.2$. The rescaled parameters are presented in Table 2.

Table 2: Parameters Rescaled by energy optimization level

Parameter	Symbol	Value
Resistance at terminals	R_1	$0.03(1-0.8p_{Popt})$
Resistance to C_2	R_2	$0.03(1-0.8p_{Popt})$
Resistance to C_3	R_4	$0.04(1-0.8p_{Popt})$
Mass per kWh	m	$7(1+p_{Popt}^2+10p_{Popt}^{20})$ kg/kWh
Battery cost per kWh	c_{batt}	$200(1+p_{Popt}^2+10p_{Popt}^{20})$ EUR/kWh
Scaling for degradation by voltage and current	p_{d5}	$1(1-0.5p_{Popt})$ p.u./year

2.6 Sanity check of the model

While the model parameters have not yet been systematically optimized to fit the model to any data set for battery life and are mainly intended to illustrate a proposed model structure for this type of studies, it is still relevant to verify that the model gives reasonable results. Figure 3a shows the battery life predicted by the model when exposed to simple cycling similar to a typical cycling test in a laboratory. The general shape and orders of magnitude agree with expectations. In this case, 0.3 C charging/discharging results in most cycle life and therefore also most cycled energy. At 0.1 C, the battery has less cycle life due to calendar aging, and at higher C-rates the current-dependent degradation mechanisms reduce the cycle life.
Figure 3b shows the battery life predicted by the model when exposed to simple cycling around different average SOC levels and with different SOC ranges. Unlike the previous figure, this figure is scaled in full-cycle equivalences. The highest predicted cycle life is given for SOC average around 0.2 p.u. and a small SOC range, as expected. At 100% SOC cycles at 1 C, centered around 50% , the predicted battery life is 2500 cycles.
Figure 4 compares the model result with a publicized set of cycling experiments. [4] It can be seen that the battery life is predicted to be within a factor of 2 in most cases. We hope that much better future predictions will be possible by properly fitting the model parameter to available data.

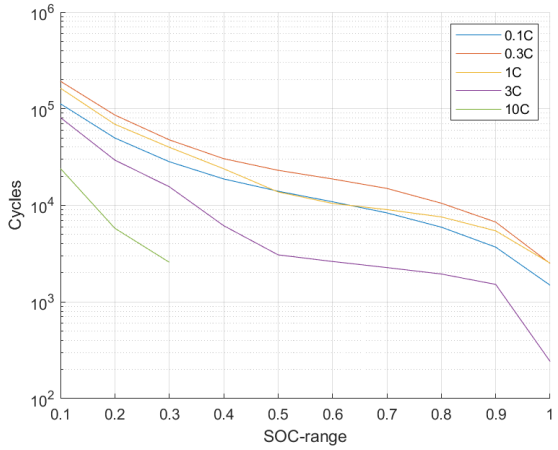

(a) Predicted battery life in full cycle equivalents with EOL at 80% capacity, for simple cycling at different cycle depths and C-rates. Average SOC-level is selected to maximize battery life.

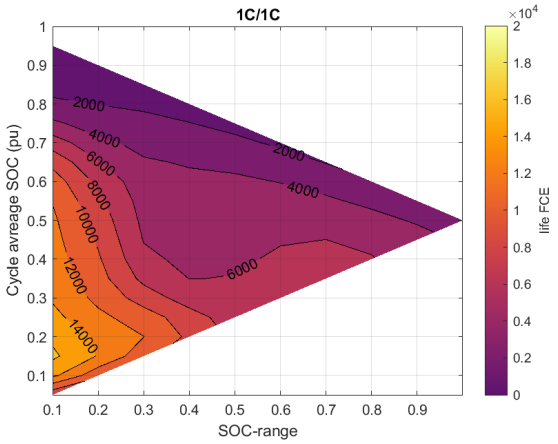

(b) Predicted battery life in full cycle equivalents with EOL at 80% capacity, for simple cycling at a C-rate of 1 for both charging and discharging

Figure 3: Model results for simple cycles.

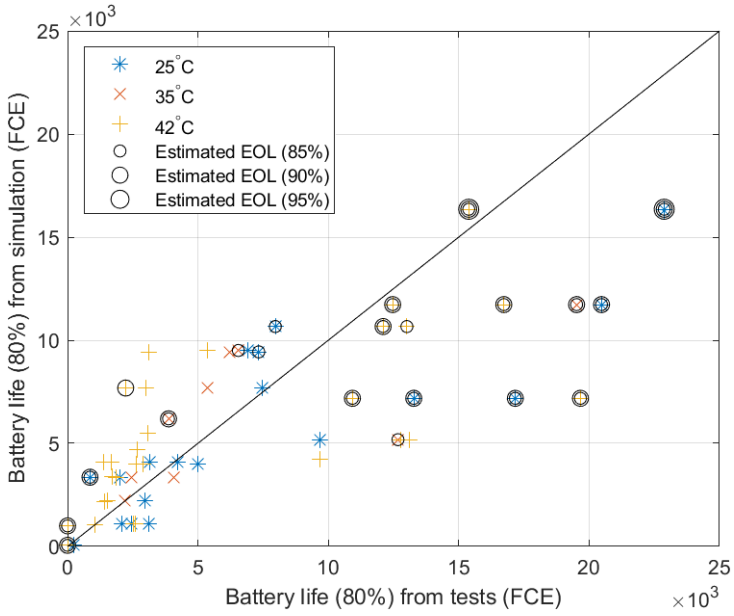

Figure 4: Comparison between predicted cycle life by the model and the estimated cycle life based on published results [4]. A full description of these cases is beyond the scope of this article. The different points represent test cycles with different SOC ranges and C-rates of 1,2 and 4. The points that are encircled are tests where the battery did not degrade to 80% during the test, the value shown for these points are extrapolated to the number of cycles that would be required to reach 80% remaining capacity at constant degradation rate.

3 Examples of different charging infrastructure for Long-haul trucks

Table 3 and Figure 5 present four example cases in which a long-haul truck performs the same transport task but uses different charging infrastructure. The power demand in these examples comes from a simulation of driving a 40-ton truck the 563 km from Helsingborg to Stockholm in Sweden with an rather high average energy consumption of 1.91 kWh/km. To make it simple, it is assumed that all days are the same and that it only makes one trip per day. The battery is slow charged for 8 hours at night, presumably in the depot with a power selected to reach the same SOC as the day started with. The cases are as follows.

- Using only the charger in the depot without extra charging during the day. This will result in a large, expensive, and heavy battery, but minimizes the cost of the charging infrastructure.
- Fast charging during lunch break with 800 kW and depot charging. This is probably the most likely case for operation in the near future.
- Electric road system (ERS). This is a system that supplies power to vehicles while driving, either inductively or through sliding contacts. It is often more economical to build shorter ERS with higher power rather than building the entire distance.

  The road was divided into 650-meter sections (30 seconds driving). The 15 % of the sections where the average power consumption is greater than 243 kW had ERS installed, capable of delivering 800 kW. This means that ERS is installed mainly in uphill sections.
- Fast ch. 5 min every 75 km. In a future with self-driving vehicles, driving and rest-time rules will be irrelevant. It may therefore be more economical to make shorter charging stops, but more frequent. Since batteries in general are better at handling high power for short periods, the charging power is set to 1200 kW instead of 800 kW.

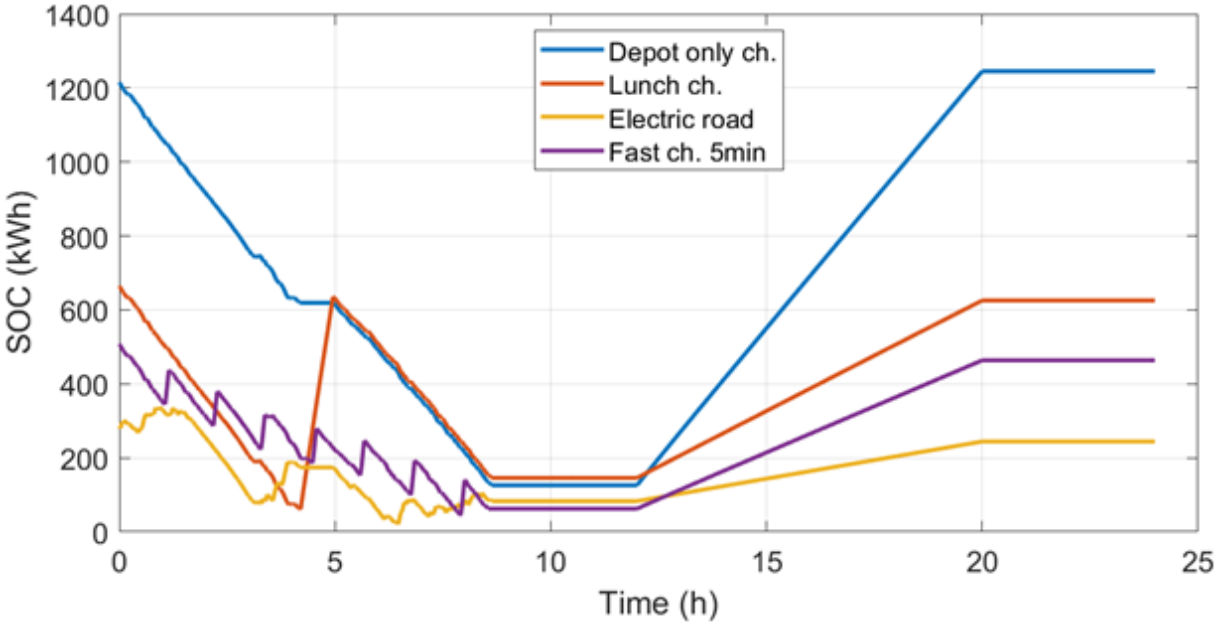

Figure 5: The battery energy content for the different cases. The time is relative to the start of the transport task.

Table 3: The example cases. All cases consist of a 40-ton truck driving 563 km.

Case	Depot charging only	Lunch charging	Electric road	Fast ch. 5 min every 75 km
Slow charging 8 h @ (kW)	140	60	20	50
Fast charging power (kW)	-	800	-	1200
Number of fast chargers	0	1	0	7
Total fast charging time (minutes) -	-	45	-	35
Electric road power (kW)	-	-	800	-
Electric road coverage (%)	0	0	15	0

Table 4: Optimized batteries for the example cases. All cases consist of a 40-ton truck driving 563 km.

Case	Depot charging only	Lunch charging	Electric road	Fast ch. 5 min every 75 km
Battery Capacity (kWh)	1519	811	440	627
Power ($p_{Popt} = 1$) or energy ($p_{Popt} = 0$) optimized, (p_{Popt})	0.069	0.19	0.15	0.14
Battery mass (kg)	10700	5900	3100	4500
Used SOC window (%)	74	74	72	74
Max charging C-rate including regenerative braking (kW/kWh capacity)	0.11	0.99	1.27	1.91
Economic battery life (years)	10.5	7.6	9.6	9.7
Battery related costs (EUR/km)	0.48	0.30	0.16	0.23
How much more the charging infrastructure may cost relative to "Depot charging only" for break even (EUR/vehicle/year)	Reference case	37 000	66 000	51 000

4 Results

The results of the model are shown in Table 4. In each case, an optimization algorithm (fminsearch in MATLAB) has selected the battery capacity, the power optimization level, and the initial state of charge (SOC) to minimize battery-related costs.
Given the limited validation and calibration of the model, all these results should be seen as an illustration of the principles and how this type of model can be used rather than as facts.
The *Used SOC window* only varies from 72 to 74 % between the cases, but this is probably just a coincidence.
We can see that the case with Lunch charging requires the most power-optimized battery according to this model. This is because long fast-charging sessions are the most demanding, even if the C-rate is higher in Cases 3 and 4.

Battery-related costs include battery investment with interest, energy loss in the batteries, and the cost of lost payload capacity due to battery mass.
The battery-related costs are lowest in the case of electric road, 0.24 EUR/km cheaper than depot charging, but a large part of this cost reduction can be gained by the much simpler lunch charging.
These costs can be combined with the cost of the different charging infrastructures and other costs to compare the total cost of the system of the different solutions.
The maximum infrastructure cost for break even against *Depot charging only* is shown in the last row of Table 4, expressed as EUR per vehicle and year. Whether a case can become profitable compared to the other cases depends not only on this break-even cost, but also on how many vehicles can share the infrastructure.

5 Conclusions

A model structure is presented that makes it feasible to compare battery-related costs for widely different charging solutions, including solutions with highly dynamic and complex charging patterns such as electric roads.
Together with cost estimates for the charging solutions themselves, this makes it possible to compare the cost of different solutions in an early concept evaluation stage, before vehicles that fit the application may even have been developed.
All models have a trade-off between complexity and approximations; we are not aware of any other model that fits the same niche, even though there are many other battery aging models, both simpler and more detailed.
This model helps to compare different solutions on technical grounds regardless of what types of vehicle currently are in mass production.
The parameter values presented give reasonable results and can be used to demonstrate the principles, but further calibration and validation of the parameter values is needed before qualitative results can be trusted.

6 Future work

- Further calibrate and validate the model against experimental aging data.
- Implement automatic optimization of the charging , to minimize battery damage.
- Expand the range of example cases and try to compare different applications, such as haul trucks, buses, boats, and airplanes.
- Integration with more detailed total cost of ownership (TCO) model.

Acknowledgments

Oscar Lind Jonsson at Linköping University has kindly provided the simulated battery power time series for a trip from Helsingborg to Stockholm that is used in this work.

References

[1] L. Lindgren, A. Grauers, J. Ranggård, and R. Mäki, "Drive-cycle simulations of battery-electric large haul trucks for open-pit mining with electric roads," *Energies*, vol. 15, no. 13, p. 4871, 2022.

[2] L. Lindgren, *Full electrification of Lund city bus traffic - A simulation study*. Department of Industrial Electrical Engineering and Automation, Lund Institute of Technology, 2015, vol. 7255.

[3] ASTM, "Standard practices for cycle counting in fatigue analysis," 2017, aSTM standard E1049-85(2017). [Online]. Available: "https://compass.astm.org/document/?contentCode=ASTM%7CE1049-85R17%7Cen-US"

[4] E. Wikner, "Ageing in commercial li-ion batteries: Lifetime testing and modelling for electrified vehicle applications," Ph.D. dissertation, Chalmers University, 2019.

Presenter Biography

Lars Lindgren holds a B.Sc. in Electrical Engineering and Computer Science from Malmö University and a Licentiate from Lund University focused on power system restoration after blackouts. He has worked as a research engineer at Lund University, contributing to electric road research, among other projects. Currently, he is a Ph.D. student at Chalmers University, researching the electrification of long-haul trucks.